Int. J. Electron. Commun. (AEÜ) 68 (2014) 1–9

Contents lists available at ScienceDirect

International Journal of Electronics and Communications (AEÜ)

journal homepage: www.elsevier.com/locate/aeue

CCII based more tunable voltage-mode all-pass filters and their quadrature oscillator applications

Firat Yucel [a], Erkan Yuce [b,*]

[a] Department of Informatics, Akdeniz University, 07059 Konyaalti-Antalya, Turkey
[b] Department of Electrical & Electronics Engineering, Pamukkale University, 20070 Kinikli-Denizli, Turkey

ARTICLE INFO

Article history:
Received 6 May 2013
Accepted 27 June 2013

Keywords:
All-pass filter
CCII
CMOS
Quadrature oscillator

ABSTRACT

In this paper, two new voltage-mode (VM) first-order all-pass filters using single active element namely second-generation current conveyor (CCII) and a grounding capacitor are proposed. The first proposed filter employs a dual output CCII (DO-CCII) and the other one uses a modified minus type CCII (MCCII−). One of the main advantages of both configurations is their high input impedances; thus, both can be easily cascaded with other VM circuits. Additionally, the use of a grounded capacitor in both circuits provides suitability for integrated circuit (IC) fabrication process. However, both of the proposed circuits need a single passive component matching constraint. Non-ideality analysis is performed for the proposed circuits. Moreover, two quadrature oscillator applications of the proposed filters are given. The behavior of the filters is verified by SPICE simulations. Also, experimental tests using commercially available ICs (AD844s) are achieved for the second proposed configuration.

© 2013 Elsevier GmbH. All rights reserved.

1. Introduction

All-pass filters (APFs) [1–32] are widely used in many applications to change the phase of electrical signal while keeping the amplitude of the signal constant. The property of high-input impedance is significant for voltage-mode (VM) active filters. VM APFs can be implemented using various active building blocks (ABBs) such as second generation current conveyor (CCII) which was introduced by Sedra and Smith [33]. The use of CCIIs in some circuit topologies provides high performance and functional versatility [34].

In the literature, there are some VM APF topologies using single ABB [1–7,10,11,15,17,19,21,22,25–32] such as CCII, voltage differencing-differential input buffered amplifier (VD-DIBA), differential buffered and transconductance amplifier (DBTA), voltage differencing inverting buffered amplifier (VDIBA), universal voltage conveyor (UVC), differential voltage current conveyor (DVCC), differential difference current conveyor (DDCC), fully differential current conveyor (FDCCII), differential CCII (DCCII), inverting current differencing buffered amplifier (ICDBA), current controlled current differencing buffered amplifier (C-CDBA), dual-X second-generation current conveyor (DXCCII), differential difference amplifier (DDA), variable gain current conveyor (VGCCII), and inverting voltage buffer (IVB). However, some APFs [5,10,11,15,19–21,26,27,29,31,32] do not have the feature of high input impedance. Also, several APFs [4–6,10,11,19–21,23,29–31] do not contain a grounded capacitor. Some APFs [18,22,23,25] have a capacitor connected in series to the X-terminal of the active device; thus, their high frequency performances are not well [35]. Some APFs [23,25,26] do not employ a canonical number of capacitors (only one). A number of APFs [8,9,12–14,16,18,20,23,24] use more than one ABB. The cascadable APF employing a dual output CCII (DO-CCII) in [1] does not have a resistor connected in series to the X-terminal of the DO-CCII. Another APF configuration using a modified minus-type CCII (MCCII−) does not have a resistor connected in series to the X-terminal of the MCCII−. Therefore, two electronically tunable floating resistors [36] should be replaced instead of resistors of the circuits in [1,2] to control externally. Fortunately, if second-generation current-controlled current conveyors (CCCIIs) [37] are replaced instead of both of the proposed circuits, the resistors connected to the X terminal of the CCCIIs are removed and a floating tunable resistor is replaced instead of each of the other resistors, both of the proposed circuits can be tuned externally.

In this paper, two CCII based VM APF configurations are proposed. One of the proposed APFs uses a DO-CCII and the other one employs a MCCII−. One of the main properties of the proposed APFs is their high input impedances; thus, they can be easily cascaded with other VM circuits. Also, both of the proposed APFs are composed of a grounded capacitor; accordingly, they are suitable for integrated circuit (IC) fabrication [38]. Nevertheless, both of the

* Corresponding author. Tel.: +90 536 689 41 21.
E-mail addresses: fyucel@akdeniz.edu.tr (F. Yucel), erkanyuce@yahoo.com (E. Yuce).

1434-8411/$ – see front matter © 2013 Elsevier GmbH. All rights reserved.
http://dx.doi.org/10.1016/j.aeue.2013.06.012

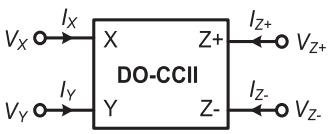

Fig. 1. Electrical symbol of the DO-CCII.

proposed APFs need a single resistive matching condition. Further, two quadrature oscillators derived from the proposed APFs are given as application examples. Non-ideality analysis is performed for the proposed APFs. A number of simulation results are included to confirm to theory. Moreover, experimental test results are given.

The paper is organized as follows: After introduction is given in Section 1, DO-CCII and MCCII− are treated in Section 2. Proposed APF structures are given in Section 3. In Section 4, parasitic impedance effects on the proposed APFs are investigated. As application examples, two quadrature oscillators are given in Section 5. Simulation and experimental test results for the APF topologies are, respectively, given in Sections 6 and 7. In Section 8, some conclusion remarks are given.

2. Circuit description

One of the proposed circuits in this paper employs a single DO-CCII and the other one uses a single MCCII−. Electrical symbol of DO-CCII with four terminals is depicted in Fig. 1. MCCII− with three terminals, which has the current gain (γ) less than unity and greater than zero, can be obtained by grounding $Z+$ terminal of DO-CCII. Also, the current gain at the Z terminal of the MCCII− can be adjusted by changing relevant aspect ratios of the CMOS transistors of the DO-CCII in Fig. 2 [37].

The DO-CCII can be presented with the following matrix equation:

$$\begin{bmatrix} V_X \\ I_Y \\ I_{Z+} \\ I_{Z-} \end{bmatrix} = \begin{bmatrix} \beta & 0 \\ 0 & 0 \\ 0 & \alpha \\ 0 & -\gamma \end{bmatrix} \begin{bmatrix} V_Y \\ I_X \end{bmatrix} \tag{1}$$

where α and γ are frequency dependent non-ideal current gains and β is frequency dependent non-ideal voltage gain, which are all ideally equal to unity. α, β and γ at sufficiently low frequencies can be presented as $\alpha = 1 - \varepsilon_\alpha$ ($|\varepsilon_\alpha| \ll 1$), $\beta = 1 - \varepsilon_\beta$ ($|\varepsilon_\beta| \ll 1$) and $\gamma = 1 - \varepsilon_\gamma$ ($|\varepsilon_\gamma| \ll 1$) where ε_α and ε_γ are current tracking errors and ε_β is voltage tracking error, which are all ideally equal to zero.

3. The proposed APFs

In this section, two voltage-mode first-order APF structures are introduced. One of them shown in Fig. 3 is implemented by using only one DO-CCII, two resistors ($R_2 = R_1$) and a grounded capacitor (C_1).

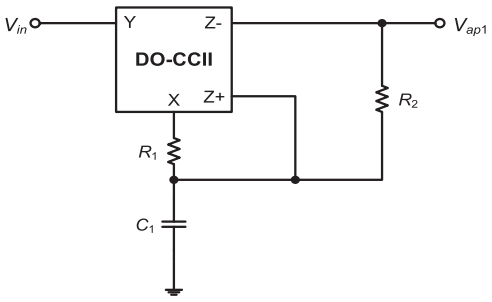

Fig. 3. Circuit schematic of the first proposed all-pass filter.

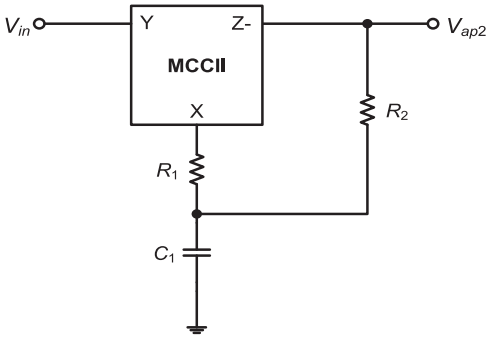

Fig. 4. Circuit schematics of the second proposed all-pass filter.

Transfer function (TF) of the first proposed filter in Fig. 3 with $R_1 = R_2 = R$ can be ideally written as

$$\frac{V_{ap_1}}{V_{in}} = \frac{1 - sC_1R}{1 + sC_1R} \tag{2}$$

which provides non-inverting all-pass responses. Here, the angular resonance frequency (ω_o) of the first proposed filter is found as $1/(C_1R)$. Also, the phase response is evaluated as follows:

$$\varphi(\omega) = -2\tan^{-1}(\omega C_1 R) \tag{3}$$

where the phase changes from 0° to −180° as the frequency varies from zero to infinity. The TF of the circuit in Fig. 3 with non-ideal gains is obtained as follows:

$$\frac{V_{ap_1}}{V_{in}} = \beta\frac{1 + \alpha - \gamma - s\gamma C_1 R_2}{1 + \alpha - \gamma + sC_1 R_1} \tag{4}$$

Here, the phase response of the proposed filter can also be obtained as

$$\varphi(\omega) = -\tan^{-1}\frac{\omega\gamma C_1 R_2}{1 + \alpha - \gamma} - \tan^{-1}\frac{\omega C_1 R_1}{1 + \alpha - \gamma} \tag{5}$$

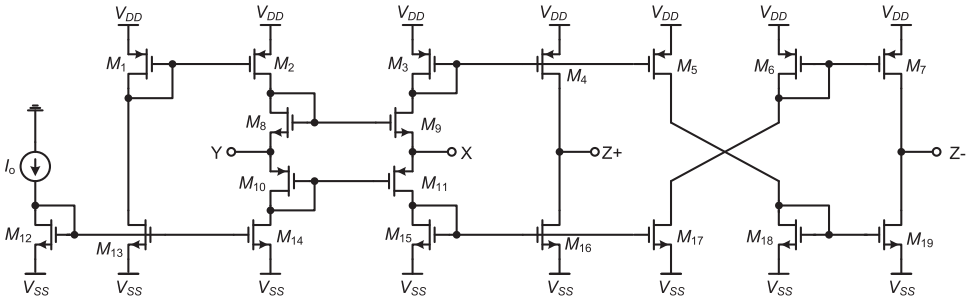

Fig. 2. Internal structure of the DO-CCII [37].

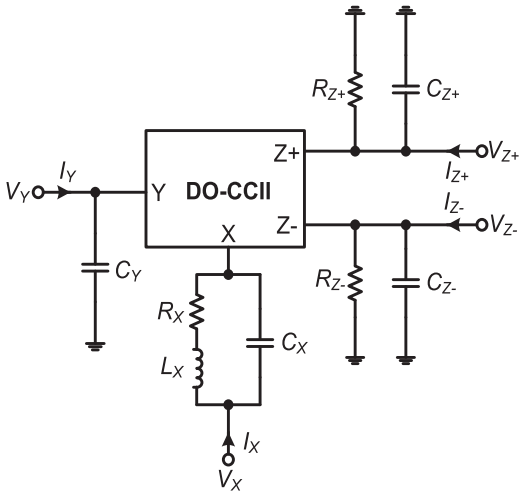

Fig. 5. DO-CCII with parasitic impedances.

The second proposed APF configuration is seen in Fig. 4. It consists of only one MCCII−, two resistors ($R_2 = R_1/\gamma$ and $0 < \gamma < 1$) and a grounded capacitor (C_1).

The TF of the second proposed APF in Fig. 4 is the same as given in Eq. (2) if $R_2 = 2R_1$ and $\gamma = 0.5$ is chosen. Also, the following TF of the second proposed circuit in Fig. 4 with non-ideal gains is obtained:

$$\frac{V_{ap_2}}{V_{in}} = \beta \frac{1 - s(\gamma C_1 R_2)/(1-\gamma)}{1 + s(C_1 R_1)/(1-\gamma)} \tag{6}$$

where phase response of the APF can be obtained as

$$\varphi(\omega) = -\tan^{-1}\frac{\omega\gamma C_1 R_2}{1-\gamma} - \tan^{-1}\frac{\omega C_1 R_1}{1-\gamma} \tag{7}$$

4. Influence of the parasitic impedances

A DO-CCII with parasitic impedances is given in Fig. 5. Since C_X is effective only high frequencies, its effect can be neglected. For the first proposed APF, if only X-terminal parasitic impedances are taken into account, the following TF is obtained:

$$\frac{V_{ap_1}}{V_{in}} = \frac{1 - sC_1R_2}{1 + sC_1(R_1 + R_X + sL_X)} \tag{8}$$

where R_X and L_X are the parasitic impedances of the DO-CCII. If only Z-terminal parasitic impedances are considered, the TF of the first proposed filter can be rewritten as follows:

$$\frac{V_{ap_1}}{V_{in}} = \frac{R_{Z-}(R_{Z+} - R) - sRR_{Z+}(C_1 + C_{Z+})}{a_0 + a_1 s + a_2 s^2} \tag{9}$$

Here, $R_1 = R_2 = R$ is chosen and the coefficients of the denominator are found as

$$a_0 = R^2 + RR_{Z-} + 3RR_{Z+} + R_{Z-}R_{Z+} \tag{10a}$$

$$a_1 = C_{Z-}R^2R_{Z-} + C_1R^2R_{Z+} + C_{Z+}R^2R_{Z+} + C_1RR_{Z-}R_{Z+} + 3C_{Z-}RR_{Z-}R_{Z+} + C_{Z+}RR_{Z-}R_{Z+} \tag{10b}$$

$$a_2 = C_1C_{Z-}R^2R_{Z-}R_{Z+} + C_{Z-}C_{Z+}R^2R_{Z-}R_{Z+} \tag{10c}$$

For proper operation of the first proposed APF, the following constrains should be satisfied:

$$\omega L_X \ll R_1 + R_X \tag{11a}$$

$$\omega^2 a_2 \ll a_0 \tag{11b}$$

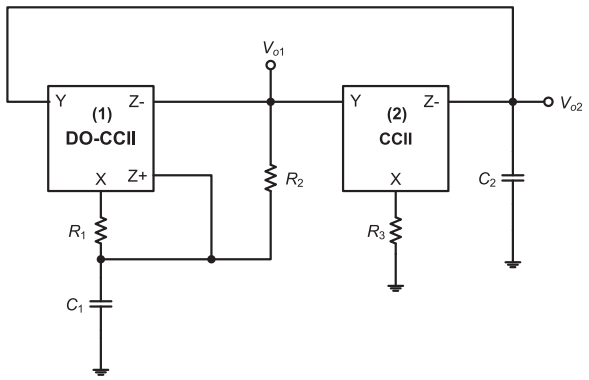

Fig. 6. The quadrature oscillator application of the first proposed circuit.

$$\omega a_2 \ll a_1 \tag{11c}$$

From Eqs. (11), the following operating frequency ranges are obtained:

$$f \le \frac{0.1(R_1 + R_X)}{2\pi L_X} \tag{12a}$$

$$f \le \sqrt{\frac{0.1a_0}{4\pi^2 a_2}} \tag{12b}$$

$$f \le \frac{0.1a_1}{2\pi a_2} \tag{12c}$$

If only X-terminal parasitic impedances are included, the TF for the second proposed APF is the same as Eq. (8). Also, if only Z-terminal parasitic impedances are considered, the TF of the first proposed filter where $R_2 = 2R_1 = R$ and $\gamma = 0.5$ is given as follows:

$$\frac{V_{ap_2}}{V_{in}} = \frac{R_{Z-}(1 - C_1R)}{3R + R_{Z-} + s(C_1R^2 + C_1RR_{Z-} + 3C_{Z-}RR_{Z-}) + s^2C_1C_{Z-}R^2R_{Z-}} \tag{13}$$

For proper operation of the second proposed APF, Eq. (11a) is valid, also the following constrains should be satisfied:

$$\omega^2 C_1C_{Z-}R^2R_{Z-} \ll 3R + R_{Z-} \tag{14a}$$

$$\omega C_1C_{Z-}R^2R_{Z-} \ll C_1R^2 + C_1RR_{Z-} + 3C_{Z-}RR_{Z-} \tag{14b}$$

From Eqs. (14), the first condition is the same as given in Eq. (12a). Also the following operating frequency ranges are obtained:

$$f \le \sqrt{\frac{0.1(3R + R_{Z-})}{4\pi^2 C_1C_{Z-}R^2R_{Z-}}} \tag{15a}$$

$$f \le \frac{0.1(C_1R^2 + C_1RR_{Z-} + 3C_{Z-}RR_{Z-})}{2\pi C_1C_{Z-}R^2R_{Z-}} \tag{15b}$$

5. Quadrature oscillator applications of the proposed all-pass filters

A quadrature oscillator application of the first proposed circuit is shown in Fig. 6. It employs one DO-CCII and one CCII− as active components.

The characteristic equation for the first proposed oscillator is obtained as

$$s^2C_1C_2R_1R_3 + s(C_2R_3 - C_1R_2) + 1 = 0 \tag{16}$$

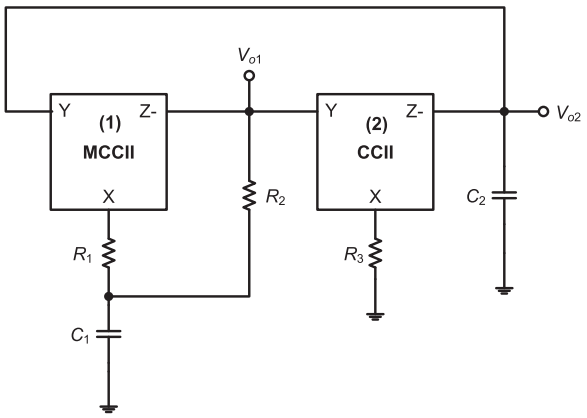

Fig. 7. The quadrature oscillator application of the second proposed circuit.

Table 1
Dimensions of the CMOS transistors.

CMOS transistors	Aspect ratios (W/L)
PMOS transistors	
M_1–M_7	41.6 μm/0.52 μm
M_{10}–M_{11}	83.2 μm/0.52 μm
NMOS transistors	
M_8–M_9	26 μm/0.52 μm
M_{12}–M_{19}	13 μm/0.52 μm

The oscillation condition (OC) of this circuit is written as

$$C_2R_3 = C_1R_2 \tag{17}$$

Oscillation frequency (f_o) of the proposed circuit is calculated as

$$f_o = \frac{1}{2\pi}\frac{1}{\sqrt{C_1C_2R_1R_3}} \tag{18}$$

For the quadrature oscillator in Fig. 6, the characteristic equation with non-ideal gains can be expressed as

$$s^2C_1C_2R_1R_3 + s(C_2R_3(1+\alpha_1-\gamma_1) - \beta_1\beta_2\gamma_1\gamma_2C_1R_2) + \beta_1\beta_2\gamma_2(1+\alpha_1-\gamma_1) = 0 \tag{19}$$

Considering non-ideal gains, the OC and the oscillation frequency f_o of the quadrature oscillator in Fig. 6 are, respectively, evaluated as follows:

$$C_2R_3(1+\alpha_1-\gamma_1) = \beta_1\beta_2\gamma_1\gamma_2C_1R_2 \tag{20a}$$

$$f_o = \frac{1}{2\pi}\sqrt{\frac{\beta_1\beta_2\gamma_2(1+\alpha_1-\gamma_1)}{C_1C_2R_1R_3}} \tag{20b}$$

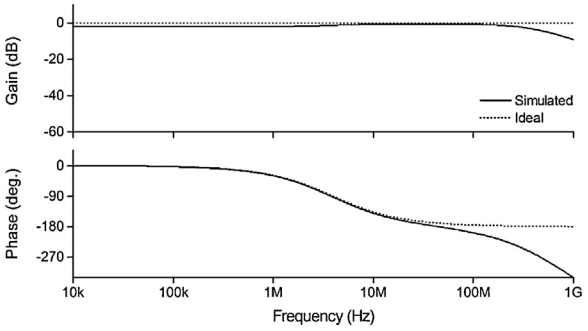

Fig. 8. Gain and phase response of the first proposed APF.

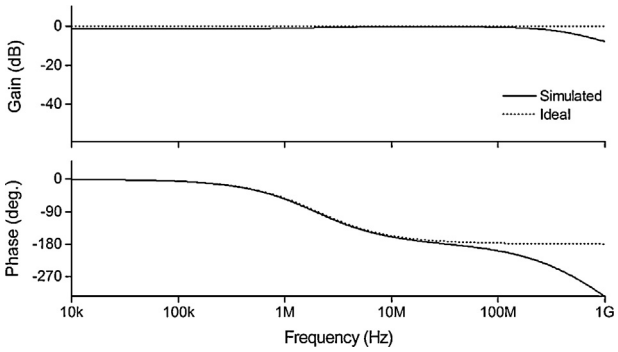

Fig. 9. Gain and phase response of the second proposed APF.

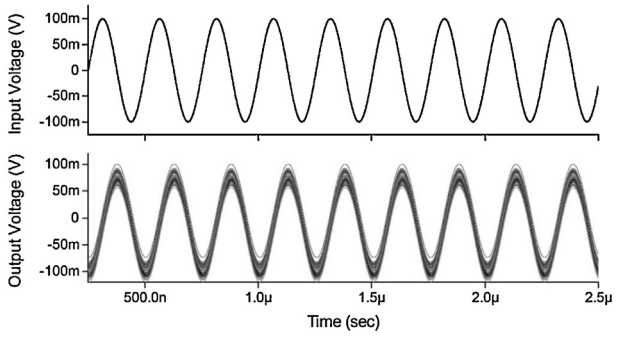

Fig. 10. Monte Carlo analysis of the first proposed filter circuit by changing V_{TH0} from 40.46 mV to 41.28 mV for NMOS transistors and from −220.1 mV to −215.6 mV for PMOS transistors.

The second quadrature oscillator application is drawn in Fig. 7. It contains one MCCII− and a CCII− as active elements. For the second proposed quadrature oscillator, the characteristic equation, OC and f_o are the same as Eqs. (16)–(18), respectively.

For the second proposed quadrature oscillator, the characteristic equation with non-ideal gains can be obtained as

$$s^2C_1C_2R_1R_3 + s(C_2R_3(1-\gamma_1) - \beta_1\beta_2\gamma_1\gamma_2C_1R_2) + \beta_1\beta_2\gamma_2(1-\gamma_1) = 0 \tag{21}$$

OC and f_o with non-ideal gains for the quadrature oscillator in Fig. 7 are, respectively, given as

$$C_2R_3(1-\gamma_1) = \beta_1\beta_2\gamma_1\gamma_2C_1R_2 \tag{22a}$$

$$f_o = \frac{1}{2\pi}\sqrt{\frac{\beta_1\beta_2\gamma_2(1-\gamma_1)}{C_1C_2R_1R_3}} \tag{22b}$$

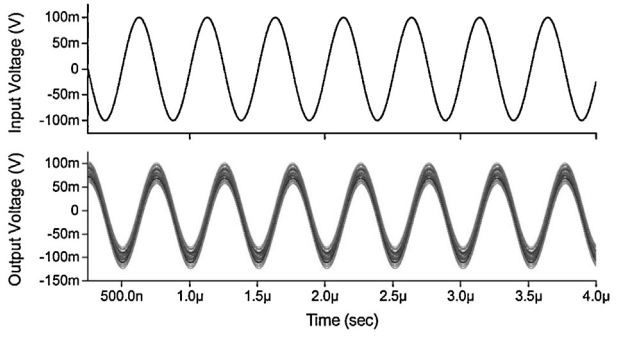

Fig. 11. Monte Carlo analysis of the second proposed filter circuit by changing V_{TH0} from 40.46 mV to 41.28 mV for NMOS transistors and from −220.1 mV to −215.6 mV for PMOS transistors.

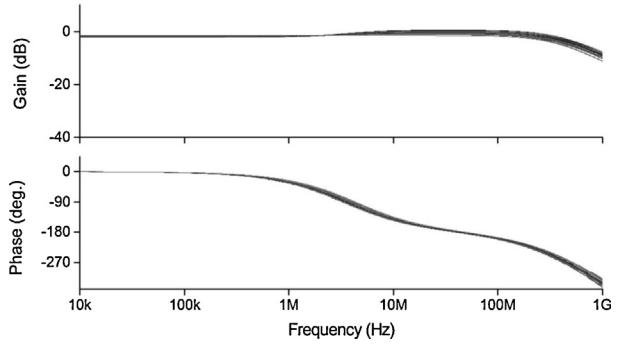

Fig. 12. Monte Carlo analysis of the first proposed filter by changing V_{TH0} from 38.83 mV to 42.92 mV for NMOS transistors and from −228.8 mV to −207 mV for PMOS transistors.

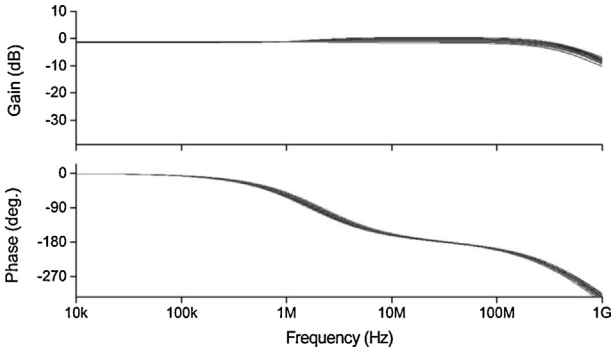

Fig. 13. Monte Carlo analysis of the second proposed filter by changing V_{TH0} from 38.83 mV to 42.92 mV for NMOS transistors and from −228.8 mV to −207 mV for PMOS transistors.

6. Simulation results

The proposed APFs and oscillator applications are simulated by using 0.13 μm IBM CMOS technology parameters [39] in SPICE program. The symmetrical power supply voltages in Fig. 2 are chosen as $V_{DD} = -V_{SS} = 0.75$ V. The bias current I_o in Fig. 2 is selected as 150 μA. The dimensions of the CMOS transistors are given in Table 1. The intrinsic resistor of the X terminal of the DO-CCII is found as R_X = 220 Ω and the value of L_X is very small.

Passive components of the first proposed APF in Fig. 3 is selected as $R_1 = 500\ \Omega$ (the effects of R_X is included), $R_2 = 500\ \Omega$ and $C_1 = 80$ pF resulting in resonance frequencies of $f_{o1} = 3.98$ MHz. Also, passive components of the second proposed APF in Fig. 4 is chosen as $R_1 = 500\ \Omega$ (the effects of R_X is included), $R_2 = 1\ \text{k}\Omega$ ($\gamma = 0.5$) and $C_1 = 80$ pF yielding resonance frequencies of $f_{o2} = 1.99$ MHz. Gain and phase response of the first and second proposed APFs in Figs. 3 and 4 are depicted in Figs. 8 and 9, respectively. From Eq. (2), gains are equal to 0 dB, whereas the gains of the proposed APFs approximately equal to −1 dB, which are acceptable. As seen from simulation results in Figs. 8 and 9, they deviate from ideal analysis when the frequency is greater than 10 MHz because of non-idealities such as frequency dependent non-ideal gains and parasitic impedances. The non-idealities of the CCII used in proposed configurations can be reduced by the methods given in

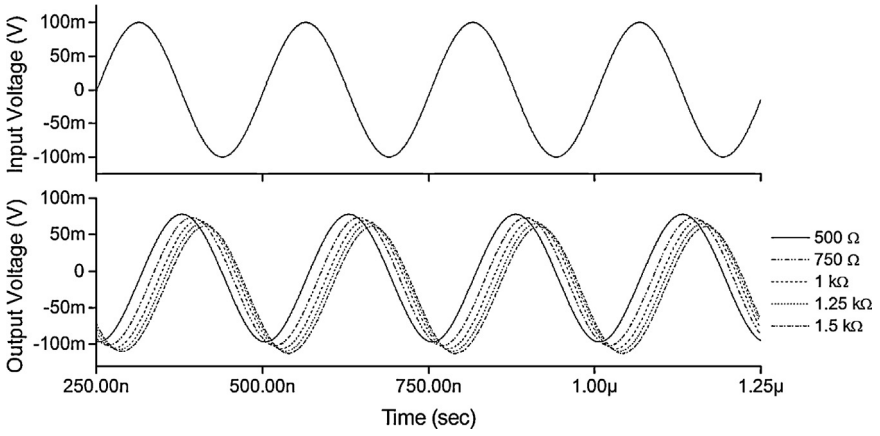

Fig. 14. The output of the first proposed APF by changing resistor values.

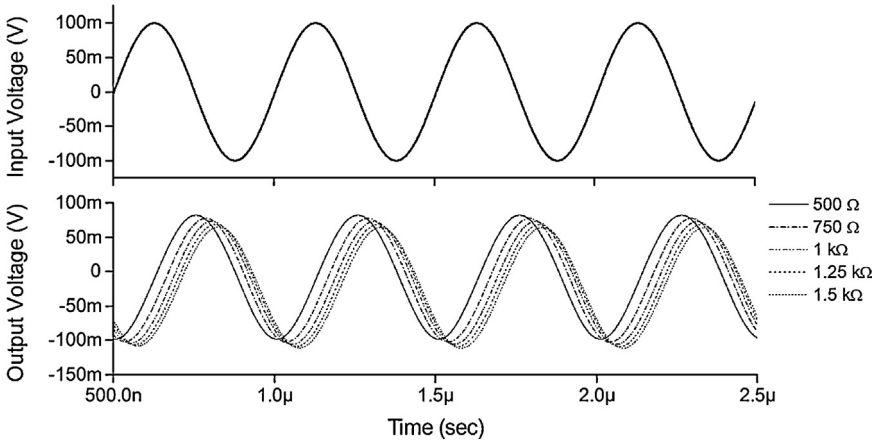

Fig. 15. The output of the second proposed APF by changing resistor values.

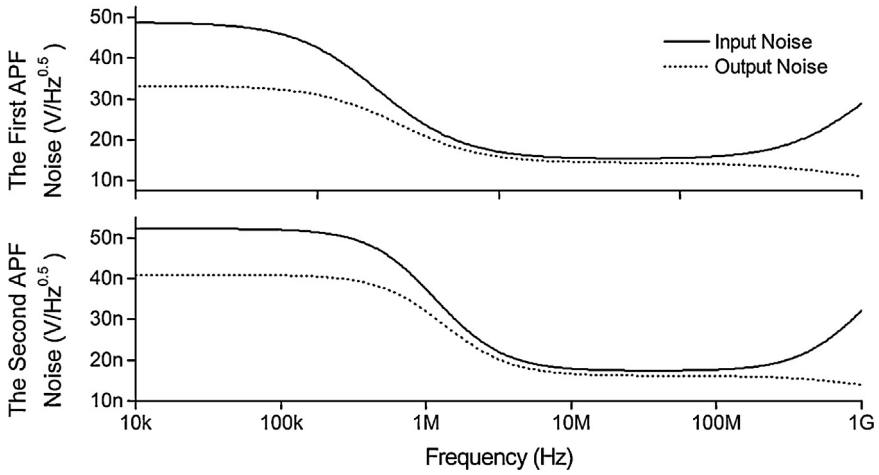

Fig. 16. The input and output noises of the first and second APFs.

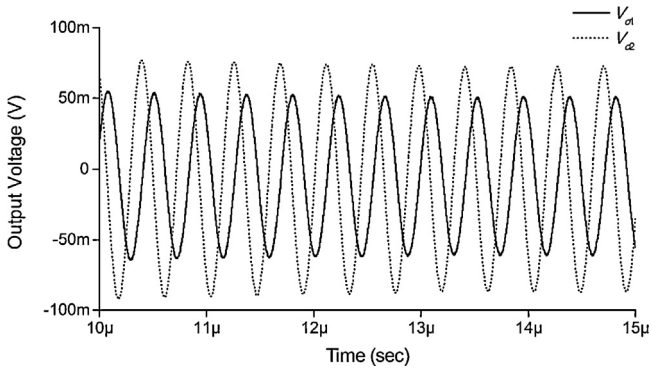

Fig. 17. Output voltages of the quadrature oscillator in Fig. 6.

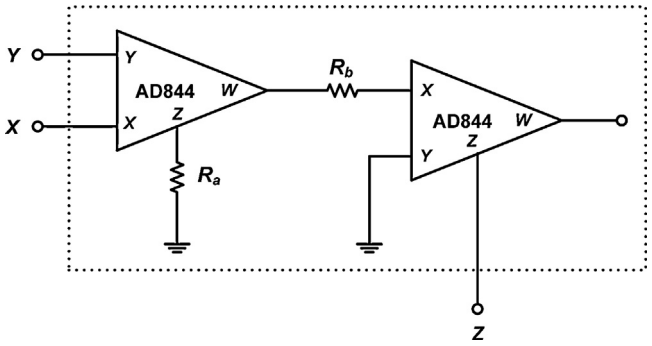

Fig. 19. The MCCII− realization using two AD844s.

[40,41]. Therefore, high frequency performance of the proposed circuits can be improved.

Monte Carlo analyses with fifty runs for 1% variations of the V_{TH0} as the standard deviations of the Gaussian distribution are performed by applying the sinusoidal input signals with peak values of 100 mV at 3.98 MHz and 1.99 MHz for the first and second proposed APFs, which are, respectively, shown in Figs. 10 and 11. It can be seen from Figs. 10 and 11 that the phases of output signals shift approximately −92° with respect to input signals whereas they are equal to −90° according to Eq. (3). The difference can be attributed to frequency depended non-ideal gain and parasitic impedance effects.

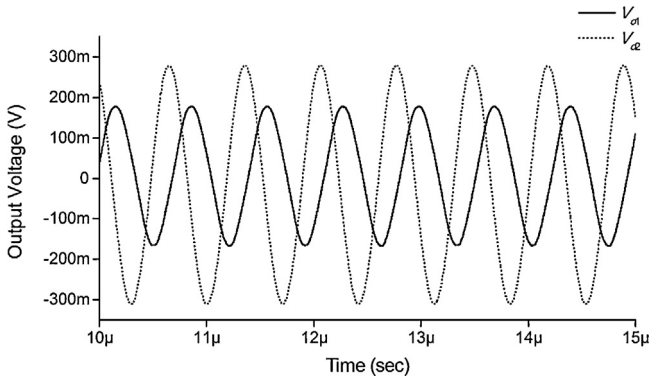

Fig. 18. Output voltages of the quadrature oscillator in Fig. 7.

To show gain and phase responses of the first and second proposed APFs, Monte Carlo analyses with fifty runs for 5% V_{TH0} variations as the standard deviations of the Gaussian distribution are given in Figs. 12 and 13, respectively.

Sinusoidal input signals with peak values of 100 mV for the first ($R_2 = R_1$) and second ($R_2 = 2R_1$ and $\gamma = 0.5$) APFs at resonance frequencies are applied where the values of R_1 are varied between 500 Ω and 1.5 kΩ, which are, respectively, illustrated in

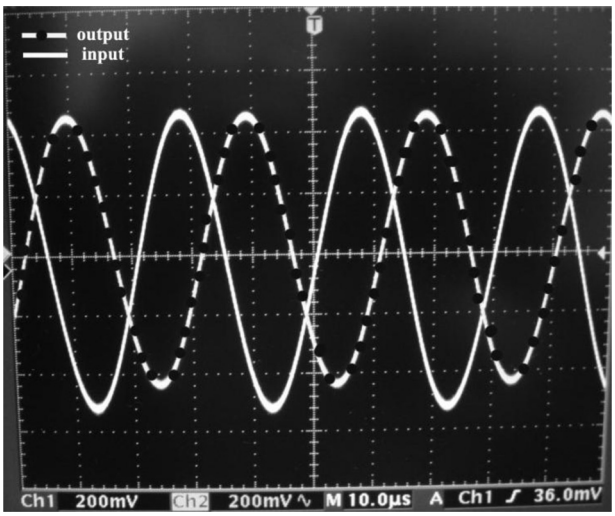

Fig. 20. Time domain experimental test results.

Table 2
A comparison table of APF circuits in open literature.

References	Active device type	# of active device	# of total transistors	Power consumption (mW)	# of grounded capacitors (total # of capacitors)	Resonance frequency	High input/low output impedance	Technology	Supply voltages (V)
[1]	DO-CCII	1	23	–	1 (1)	1 MHz	Yes/no	TSMC 0.35 μm	±1.5
[2]	MCCII–	1	21	–	1 (1)	1 MHz	Yes/no	TSMC 0.35 μm	±2.5
[3]	VD-DIBA	1	[a]	–	1 (1)	≅318 kHz	Yes/yes	OPA860. AD8130	±5
[4]	DBTA	1	[a]	–	0 (1)	≅1 MHz	Yes/yes	OPA860	±5
[5]	VDIBA	1	6	10.5	0 (1)	≅9.5 MHz	No/yes	TSMC 0.18 μm	±0.9
[6]	UVC	1	40	5.84	0 (1)	[b]	Yes/yes	TSMC 0.35 μm	±2.5
[7]	DVCC	1	18	–	1 (1)	1.59 MHz	Yes/no	TSMC 0.35 μm	±1.65
[8] Fig. 3	DDCC	2	24	–	1 (1)	1.59 MHz	Yes/no	TSMC 0.25 μm	±1.25
[9]	DVCC	2	24	1.32	1 (1)	≅1.59 MHz	Yes/yes	TSMC 0.25 μm	±1.25
[10]	DDCC	1	36	–	0 (1)	1.59 MHz	No/no	MIETEC 0.5 μm	±2.5
[11]	ICCII	1	16	–	0 (1)	370 kHz	No/no	MIETEC 0.5 μm	±2.5
[12]	OTA+DA	2	22	–	1 (1)	[b]	Yes/yes	TSMC 0.35 μm	±2.5
[13]	OTA	3	12	–	1 (1)	[b]	Yes/no	MOSIS 0.5 μm	±3
[14]	DDCC	2	24	–	1 (1)	33.84 kHz	Yes/yes	0.5 μm	±2
[15]	FDCCII	1	PSPICE model	–	1 (1)	79.6 kHz	No/no	PSPICE model	PSPICE model
[16]	DVCC	2	24	–	1 (1)	1.59 MHz	Yes/yes	0.5 μm	±2.3
[17]	DCCII	1	21	–	1 (1)	≅398 kHz	Yes/no	TSMC 0.35 μm	±2.5
[18]	DDCC	2	44	–	1 (1)	≅159 kHz	Yes/no	TSMC 0.35 μm	±1.5
[19]	ICDBA	1	30	–	0 (1)	[b]	No/yes	TSMC 0.35 μm	±2.5
[20]	C-CDBA	2	56	[b]	0 (1)	[b]	No/yes	TSMC 0.35 μm	±2.5
[21]	CCI	1	12	–	0 (1)	2.65 MHz	No/no	TSMC 0.35 μm	±2.5
[22]	FDCCII	1	44	–	1 (1)	≅1 MHz	Yes/no	0.35 μm	±1.3
[23]	CCCII+OA	2	14 + OA	–	1 (2)	12.15 kHz	Yes/yes	μA741. PR100N. NR100N	±2.5
[24]	DVCC	2	24	0.3	1 (1)	636.6 kHz	Yes/yes	TSMC 0.18 μm	±1.5
[25]	DXCCII	1	20	2.1	2 (2)	1.59 MHz	Yes/no	TSMC 0.25 μm	±1.25
[26]	FTFN	1	[a]	–	2 (2)	15.9 kHz	No/no	2× AD844	±10
[27]	DDA	1	7	–	1 (1)	1.6 MHz	No/yes	nwell 0.35 μm BiCMOS	±1.65
[28]	VGCCII–	1	28	122	1 (1)	1.59 MHz	Yes/no	TSMC 0.35 μm	±3
[29]	IVB	1	3	–	0 (1)	≅8.9 MHz	No/no	TSMC 0.13 μm	±0.65
[30]	UVC	1	40	6.54	0 (1)	390 kHz	Yes/yes	TSMC 0.35 μm	±2.5
[31]	CCII–	1	–	–	0 (1)	1 kHz	No/no	[c]	–
[32]	CCII–	1	5	0.78	1 (1)	1.59 MHz	No/no	IBM 0.13 μm	±0.75
Our work APF1	DO-CCII	1	19	1.8	1 (1)	3.98 MHz	Yes/no	IBM 0.13 μm	±0.75
Our work APF2	MCCII–	1	17	1.66	1 (1)	1.99 MHz	Yes/no	IBM 0.13 μm	±0.75

– Not given in the paper.
[a] Implemented with commercially used ICs.
[b] Variable by control voltage/current.
[c] Taken previous SPICE model of CCII.

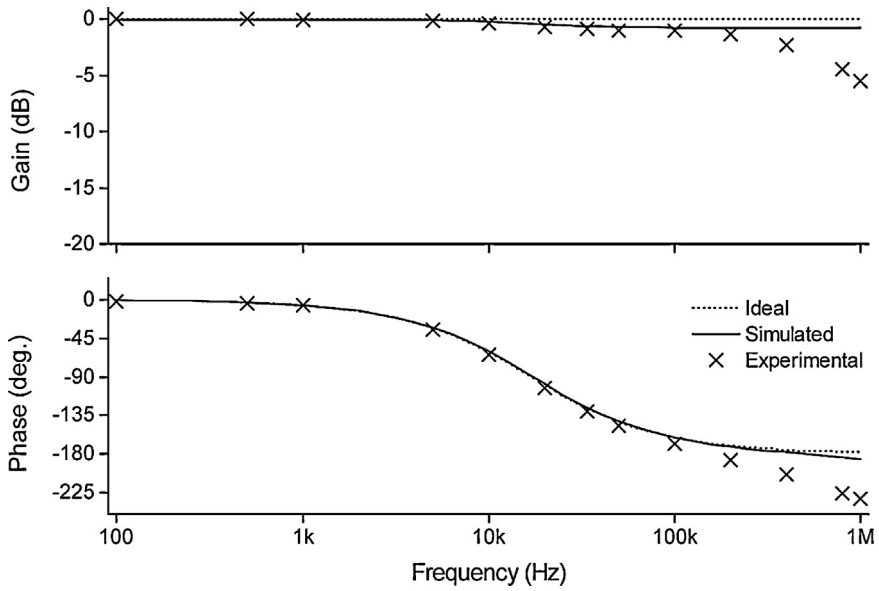

Fig. 21. Frequency domain experimental test results.

Figs. 14 and 15. From Eq. (3), if resistor values are increased, the phase shifting of output signal is expected to be higher.

The total power dissipations of the first and second APF circuits are calculated as 1.8 mW and 1.66 mW in simulations, respectively. Also, the input and output noises of the first and second APF circuits are shown in Fig. 16, which are adequately low values.

The quadrature oscillator in Fig. 6 is simulated by choosing the passive elements as $R_1 = 1\,k\Omega$ (the effects of R_X is included), $R_2 = 1\,k\Omega$, $R_3 = 600\,\Omega$ (the effects of R_X is included) and $C_1 = C_2 = 80$ pF. Also, the quadrature oscillator in Fig. 7 is simulated by choosing the passive elements as $R_1 = 1\,k\Omega$ (the effects of R_X is included), $R_2 = 2\,k\Omega$, $R_3 = 320\,\Omega$ (the effects of R_X is included) ($\gamma = 0.5$) and $C_1 = C_2 = 80$ pF. The output signals of V_{o1} and V_{o2} for Figs. 6 and 7 are depicted in Figs. 17 and 18, respectively.

Total harmonic distortions of the proposed quadrature oscillators in Figs. 6 and 7 are, respectively, found as 1.17% and 2.82% where oscillation frequencies of $f_{osc1} = 2.33$ MHz and $f_{osc2} = 1.41$ MHz calculated in SPICE simulations, which are acceptable.

7. Experimental test results

The MCCII− can be realized by using two commercially available active devices such as AD844s [42] as shown in Fig. 19 where $R_b = 2R_a = 2\,k\Omega$ is chosen. Also, $R_2 = 2R_1 = 2\,k\Omega$ and $C_1 = 4.7$ nF yielding resonance frequency of 33.86 kHz are chosen for the APF in Fig. 4 to perform experimental test. The result is demonstrated in Fig. 20 where a sinusoidal peak to peak 1 V voltage signal at 33.86 kHz is applied and $V_{CC} = -V_{EE} = 6$ V is selected. Also, ideal, simulated and experimental frequency domain responses of the proposed circuit in Fig. 4 are shown in Fig. 21. The simulated results are performed by using AD844s. The passive elements are selected as given in time-domain experimental test above. In experimental results, the phase difference between input and output signals in Fig. 20 is slightly deviated from ideal results at the resonance frequency, which is due to non-idealities of active devices, parasitics of the board and tolerances of the passive elements. Also, the difference among ideal, simulated and experimental results in Fig. 21 arises from the same reasons mentioned before.

Additionally, the ABB based first-order APF circuits in related open literature and proposed ones are compared in Table 2.

8. Conclusion

This paper presents two new VM first-order APF configurations using a single CCII and a grounded capacitor. Proposed configurations have high input impedance; therefore they are cascadable with the other VM circuits. Nevertheless, both proposed APFs require a single resistive matching constraint. Quadrature oscillator applications of the proposed APFs are also included. The proposed APF configurations and quadrature oscillators are simulated by using SPICE program. Additionally, experimental test results are included. Ideal, simulated and experimental results are close to themselves whereas the slight difference among them can be attributed to non-idealities of the CCII, tolerances of the passive elements and parasitics of the board.

Acknowledgements

We would like to thank the anonymous reviewers and associate editor for their invaluable comments for improving the paper. This work is partly funded by Pamukkale University Scientific Research Project (BAP) Management Office by grant number 2012FBE033.

References

[1] Metin B, Pal K. Cascadable allpass filter with a single DO-CCII and a grounded capacitor. Analog Integr Circuits Signal Process 2009;61:259–63.
[2] Metin B, Cicekoglu O. Component reduced all-pass filter with a grounded capacitor and high-impedance input. Int J Electron 2009;96(5):445–55.
[3] Biolek D, Biolkova V. First-order voltage-mode all-pass filter employing one active element and one grounded capacitor. Analog Integr Circuits Signal Process 2010;65:123–9.
[4] Herencsar N, Koton J, Vrba K, Metin B. Fully cascadable dual-mode all-pass filter based on single DBTA. In: 35th international conference on telecommunications and signal processing (TSP). 2012.
[5] Herencsar N, Minaei S, Koton J, Yuce E, Vrba K. New resistorless and electronically tunable realization of dual-output VM all-pass filter using VDIBA. Analog Integr Circuits Signal Process 2013;74(1):141–54.
[6] Herencsar N, Koton J, Jerabek J, Vrba K, Cicekoglu O. Voltage-mode all-pass filters using universal voltage conveyor and MOSFET-based electronic resistors. Radioengineering 2011;20(1):10–8.
[7] Horng JW. High input impedance first-order allpass, highpass and lowpass filters with grounded capacitor using single DVCC. Indian J Eng Mater Sci 2009;17:175–8.
[8] Ibrahim MA, Minaei S, Yuce E. All-pass sections with high gain opportunity. Radioengineering 2011;20(1):3–9.
[9] Ibrahim MA, Minaei S, Yuce E. All-pass sections with rich cascadability and IC realization suitability. Int J Circuit Theory Appl 2012;40:461–72.

[10] Ibrahim MA, Kuntman H, Cicekoglu O. First-order all-pass filter canonical in the number of resistors and capacitors employing a single DDCC. Circuits Syst Signal Process 2003;22(5):525–36.
[11] Ibrahim MA, Kuntman H, Ozcan S, Suvak O, Cicekoglu O. New first-order inverting-type second-generation current conveyor-based all-pass sections including canonical forms. Electrical Eng 2004;86:299–301.
[12] Keskin AU, Pal K, Hancioglu E. Resistorless first-order all-pass filter with electronic tuning. AEU Int J Electron Commun 2008;62:304–6.
[13] Kumngern M, Chanwutitum J, Dejhan K. Electronically tunable voltage-mode all-pass filter using simple CMOS OTAs. In: International symposium on communications and information technologies (ISCIT 2008). 2008.
[14] Maheshwari S, Mohan J, Chauhan DS. Cascadable all-pass and notch filter configurations employing two plus-type DDCCs. J Circuits Syst Comput 2011;20(2):329–47.
[15] Maheshwari S, Khan IA, Mohan J. Grounded capacitor first-order filters including canonical forms. J Circuits Syst Comput 2006;15(2):289–300.
[16] Maheshwari S, Mohan J, Chauhan DS. Novel voltage-mode cascadable all-pass sections employing grounded passive components. J Circuits Syst Comput 2013;22(1):1250065 (12 pp.).
[17] Metin B, Herencsar N, Vrba K. A CMOS DCCII with a grounded capacitor based cascadable all-pass filter application. Radioengineering 2012;21(2):718–24.
[18] Metin B, Pal K, Cicekoglu O. All-pass filters using DDCC- and MOSFET-based electronic resistor. Int J Circuit Theory Appl 2011;39:881–91.
[19] Metin B, Pal K, Cicekoglu O. CMOS-controlled inverting CDBA with a new all-pass filter application. Int J Circuit Theory Appl 2011;39:417–25.
[20] Metin B, Pal K. New all-pass filter circuit compensating for C-CDBA non-idealities. J Circuits Syst Comput 2010;19(2):381–91.
[21] Metin B, Cicekoglu O. Novel first order all-pass filter with a single CCI. In: IEEE Mediterranean electrotechnical conference (MELECON 2006). 2006.
[22] Metin B, Herencsar N, Pal K. Supplementary first-order all-pass filters with two grounded passive elements using FDCCII. Radioengineering 2011;20(2):433–7.
[23] Minaei S, Cicekoglu O. A resistorless realization of the first-order all-pass filter. Int J Electron 2006;93(3):177–83.
[24] Minaei S, Yuce E. Novel voltage-mode all-pass filter based on using DVCCs. Circuits Syst Signal Process 2010;29:391–402.
[25] Minaei S, Yuce E. Unity/variable-gain voltage-mode/current-mode first-order all-pass filters using single dual-X second-generation current conveyor. IETE J Res 2010;56(6):305–12.
[26] Sayginer M, Kuntman H. Realization of first-order all-pass filter using four terminal floating nullor. In: International conference on applied electronics. 2006.
[27] Toker A, Ozoguz S. Novel all-pass filter section using differential difference amplifier. AEU Int J Electron Commun 2004;58:153–5.
[28] Yuce E, Pal K, Minaei S. A high input impedance voltage-mode all-pass/notch filter using a single variable gain current conveyor. J Circuits Syst Comput 2008;17(5):827–34.
[29] Herencsar N, Koton J, Vrba K, Metin B, Cicekoglu O. Low-voltage two NMOS IVB-based voltage-mode first-order all-pass filter with tuning. In: 11th international conference on development and application systems. 2012.
[30] Metin B, Herencsar N, Koton J. Cascadable all-pass filter using a single universal voltage conveyor. In: 22nd international conference radioelektronika. 2012.
[31] Khan IA, Maheshwari S. Simple first order all-pass section using a single CCII. Int J Electron 2000;87(3):303–6.
[32] Yucel F, Yuce E. New single CCII-based first-order all-pass filters and a quadrature oscillator application. J Circuits Syst Comput 2013 (submitted for publication).
[33] Sedra A, Smith KC. A second-generation current conveyor and its applications. IEEE Trans Circuit Theory 1970;17(1):132–4.
[34] Ferri G, Guerrini NC. Low voltage, low power CMOS current conveyors. Springer; 2003.
[35] Yuce E, Minaei S. Universal current-mode filters and parasitic impedance effects on the filter performances. Int J Circuit Theory Appl 2008;36(2):161–71.
[36] Arslanalp R, Yuce E, Tola AT. Low component count BJT technology based current controlled tunable resistors and their applications. IET Circuits Devices Syst 2013;7(1):21–30.
[37] Fabre A, Saaid O, Wiest F, Boucheron C. High frequency applications based on a new current controlled conveyor. IEEE Trans Circuits Syst I Fundam Theory Appl 1996;43(2):82–91.
[38] Bhushan M, Newcomb R. Grounding of capacitors in integrated circuits. Electron Lett 1967;3(4):148–9.
[39] http://www.mosis.com/cgi-bin/cgiwrap/umosis/swp/params/ibm-013/t97f_8hp_5lm-params.txt [accessed 02.11.12].
[40] Yuce E. Negative impedance converter with reduced non-ideal gain and parasitic impedance effects. IEEE Trans Circuits Syst I Regular Pap 2008;55(1):276–83.
[41] Minaei S, Yuce E. A simple CMOS-based inductor simulator and frequency performance improvement techniques. AEU Int J Electron Commun 2012;66:884–91.
[42] Analog devices. http://www.analog.com/static/imported-files/data_sheets/AD844.pdf, AD844 datasheet (Rev. F). 2009, Doc. number: D00897-0-2/09(F).